Nonisothermal Crystallization of Polyamide 66/Poly(phenylene sulfide) Blends

Richao Zhang,[1] Yigang Huang,[2] Min Min,[1] Yong Gao,[1] Ai Lu,[1,2] Zhongyuan Lu[1]

[1]*College of Materials Science and Engineering, Southwest University of Science and Technology, Mianyang 621002, Sichuan, People's Republic of China*
[2]*Institute of Chemical Materials, China Academy of Engineering Physics, Mianyang 621900, Sichuan, People's Republic of China*

Received 1 June 2007; accepted 22 August 2007
DOI 10.1002/app.27202
Published online 13 November 2007 in Wiley InterScience (www.interscience.wiley.com).

ABSTRACT: The crystalline morphologies of isothermally and nonisothermally crystallized poly(phenylene sulfide) (PPS) and its blend with polyamide 66 (PA66) were investigated by polarized optical microscopy with a hot stage. The spherulite superstructure of PPS was greatly affected by crystallizable PA66; a Maltese cross was not clear, and the impingement between spherulites disappeared. This could be ascribed to the formation of small crystals of PA66, which filled in the PPS lamellae. The nonisothermal crystallization behavior was also measured by differential scanning calorimetry. The presence of PA66 changed the nonisothermal crystallization process of PPS. The maximum crystallization temperature of the PPS phase in the blend was higher that that of neat PPS, and this indicated that PA66 acted as a nucleus for PPS. Also, the compatibilizer poly(ethylene-*stat*-methacrylate) (EMA) was added to modify the interfacial interplay of the PA66/PPS blend system. The addition of EMA greatly influenced the nonisothermal crystallization process of the PPS phase in the blend system. © 2007 Wiley Periodicals, Inc. J Appl Polym Sci 107: 2600–2606, 2008

Key words: blends; crystallization; kinetics (polym.); miscibility; polyamides

INTRODUCTION

Poly(phenylene sulfide) (PPS) is a high-temperature thermoplastic engineering resin that was first discovered as a byproduct of the Friedel–Crafts reaction in 1888. It has a glass-transition temperature of about 80°C and a melting temperature of 280–290°C. PPS exhibits good dimensional stability, thermal stability, electrical properties, strength, fatigue resistance, and chemical resistance[1,2] and is used in widespread applications such as pump impellers, ball valves, wear rings, electrical sockets, battery and telephone components, chip carriers, optical-fiber cables, and electronic component encapsulants.[3] However, neat PPS is rather brittle, has low impact strength, and presents difficulties in injection molding. Thus, a lot of approaches have been proposed to overcome these disadvantages of PPS. The most popular method is to modify PPS by physical blending or alloying with other polymers or reinforcement with other materials. Generally, the properties of polymer blends are greatly determined by the phase morphology, dispersion, and interfacial interaction of the component polymers. In a PPS blend system, crystallizable PPS is usually blended with other polymers that are crystalline or amorphous. Hence, the morphology and ultimate properties of the products are affected by the relative crystallinity, the compatibility of the phases, and the crystallization behavior, which are determined in turn by the thermal treatment and processing conditions.

Recently, a large number of scientific publications have dealt with blends of PPS with other thermoplastics.[4–11] Golovoy et al.[4] investigated blends of PPS with polyarylate. Blends of PPS with polyethylene and poly(ethylene terephthalate) were the subjects of investigations by Nadkarni and coworkers.[5,6] PPS–poly(ether imide) and PPS–polysulfone binary blends as well as ternary systems were discussed by Akhtar and White.[7] They also described the experimental study of blends of PPS with various polyamides.[8] Hanley et al.[11] researched blends of PPS and poly (ethylene terephthalate). These studies showed that the crystallization behavior of PPS was greatly influenced by the other thermoplastics.

In this article, we characterize the crystalline morphologies and nonisothermal crystallization behavior of PPS blends with polyamide 66 (PA66). It is well known that PA66 is an important engineering thermoplastic because of its superior mechanical properties, especially when exposed to solvents at elevated temperatures.[12–18] However, PPS cannot form miscible blends with PA66, and Lee and Chun[19] found that the addition of PA66 increased the tensile strength

Correspondence to: A. Lu (ai_lu@tom.com).

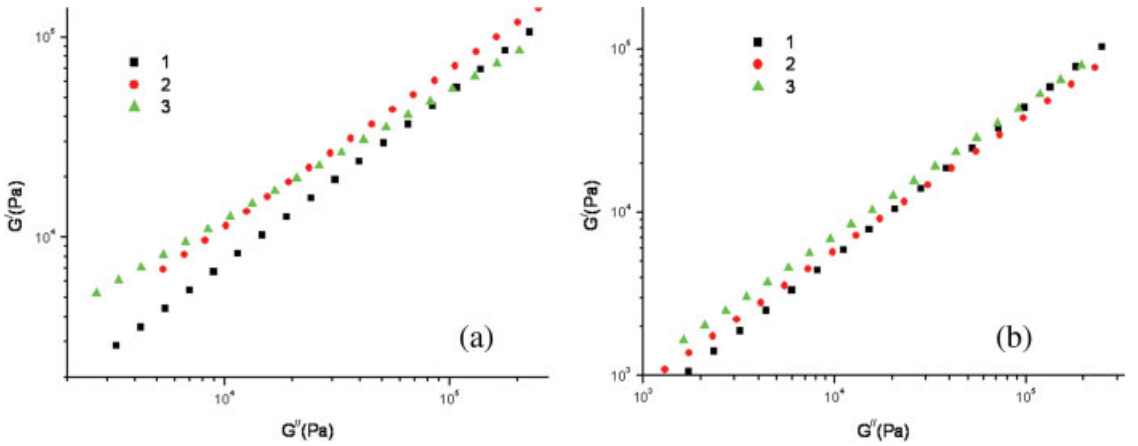

Figure 1 Relationship of log G' and log G'' for (a) PA66/PPS and (b) EMA/PA66/PPS (the weight fraction of EMA is 2%): (1) 20/80, (2) 40/60, and (3) 60/40. [Color figure can be viewed in the online issue, which is available at www.interscience.wiley.com.]

and impact strength of PPS by means of the compatibilizer poly(ethylene-*stat*-glycidyl methacrylate)-*graft*-poly(acrylonitrile-*stat*-styrene) (EGMA), which is known to improve the interfacial bonding in thermoplastic blends. Recently, some literature[20–23] has been published concerning the mechanical and physical properties of PA66/PPS blends. However, few publications have focused on the crystallization of PA66/PPS blends. As we know, the crystallization process plays an important role in the properties of PPS blends.

The aim of this work was to study the nonisothermal crystallization behavior of PPS blended with PA66. Also, poly(ethylene-*stat*-methacrylate) (EMA) was added to the PA66/PPS blends to improve their interfacial interaction.

EXPERIMENTAL

Materials and compounding

A PPS resin powder with a weight-average molecular weight of 40,000 was supplied by Honghe Limited Corp. (Zigong, China). PA66 was supplied by Shenma Group Ltd. Corp. (China). The crystallization temperature of PA66 was about 210°C. The PPS samples were first treated at 140°C for 4 h to remove the lower molecular weight ones and then blended with PA66 (in a weight ratio of 7 : 3) under a nitrogen atmosphere with a Stress Polylab610 rheometer (RS600). The molten mixing was carried out at 290°C, and the mixing time was 6 min.

After the blending with PA66 in a twin-screw compounding machine, a circular film with a 1-mm thickness and 20-mm diameter was prepared with a self-made oil pressure pump for rheological testing.

Rheological testing

The compatibility of PPS blended with different PA66 contents was determined with a Stress Polylab610 rheometer (RS600); the scanning frequency ranged from 0.01 to 100. The measurement temperature was 290°C. The data obtained are presented in Figure 1.

Differential scanning calorimetry (DSC) measurement

The nonisothermal crystallization behavior of PPS and its blend with PA66 were determined in a nitrogen atmosphere with a PerkinElmer Diamond differential scanning calorimeter. The crystallization exotherm was recorded when the samples (ca. 8 mg) were heated to 330°C, held at that temperature for 5 min to ensure complete melting of the polymer, and then cooled at a rate of 20, 15, or 10°C/min to room temperature.

Morphology observation

The crystalline morphologies of the isothermally and nonisothermally crystallized PPS and its blend with PA66 from the melt were observed with a polarized optical microscope equipped with a CSS450 hot stage. Temperature calibration of the hot stage was performed with naphthalene, indium, anthraquinone, and sodium nitrate. The samples were heated from 20 to 330°C at 20°C/min, kept at that temperature for 5 min to allow complete melting, and then cooled to the crystallization temperature at 30°C/min for isothermal crystallization and to room temperature at 20, 15, or 10°C/min for nonisothermal crystallization.

RESULTS AND DISCUSSION

Compatibility of EMA/PA66/PPS blends

Figure 1 presents the dependence of the storage modulus (G') on the loss modulus (G'') for PA66/PPS and EMA/PA66/PPS blend systems. According to the cri-

teria for the rheological compatibility of polymer blends established by Han and coworkers,[24–26] plots of G' versus G'' give composition-independent correlations for compatible blends and composition-dependent correlations for incompatible blends. It can be seen from Figure 1(a) that the plots of G' versus G'' are dependent on the composition for the PA66/PPS blend system. This phenomenon is consistent with what Han and coworkers observed in incompatible blend systems, such as nylon 6/CXA 3101 and nylon 6/poly(ethylene-*co*-vinyl acetate) (EVA) systems. Thus, we believe that PPS is incompatible with crystallizable PA66 in the melt state. In Figure 1(b), one can see that the plots of G' versus G'' are independent of the composition for the blend system, indicating that the addition of EMA greatly modifies the interfacial interaction of the PA66/PPS blend and improves the compatibility of the blend system.

Nonisothermal crystallization behavior of EMA/PA66/PPS blends

The nonisothermal crystallization exotherms of neat PPS and neat PA66 at a predetermined cooling rate of 15°C/min are shown in Figure 2. It can be seen from these DSC curves that the exothermic crystallization peaks for both neat PPS and neat PA66 are monomodal. The crystallization temperature for neat PPS and PA66 ranges from 208.85 to 243.35°C and from 201.44 to 236.18°C, respectively. The maximum crystallization peak temperature of neat PPS is about 223.85°C, and that of PA66 is about 208.7°C. These data indicate that the crystallization of PPS is before that of PA66 during cooling.

Figure 3 shows the nonisothermal crystallization exotherms of PPS, a PA66/PPS blend, and an EMA/PA66/PPS blend at predetermined cooling rates of

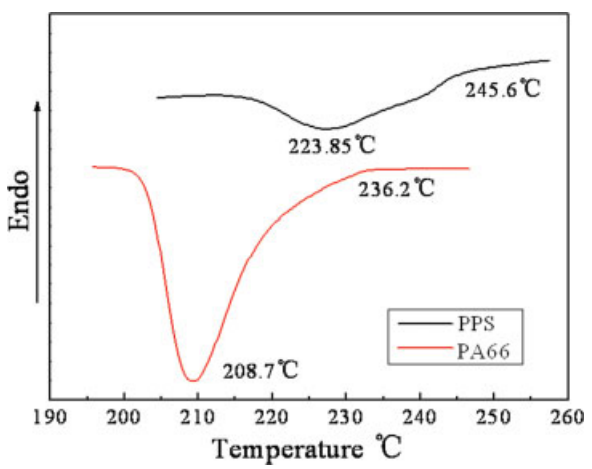

Figure 2 DSC cooling traces at a cooling rate of 15°C/min for neat PPS and neat PA66. [Color figure can be viewed in the online issue, which is available at www.interscience.wiley.com.]

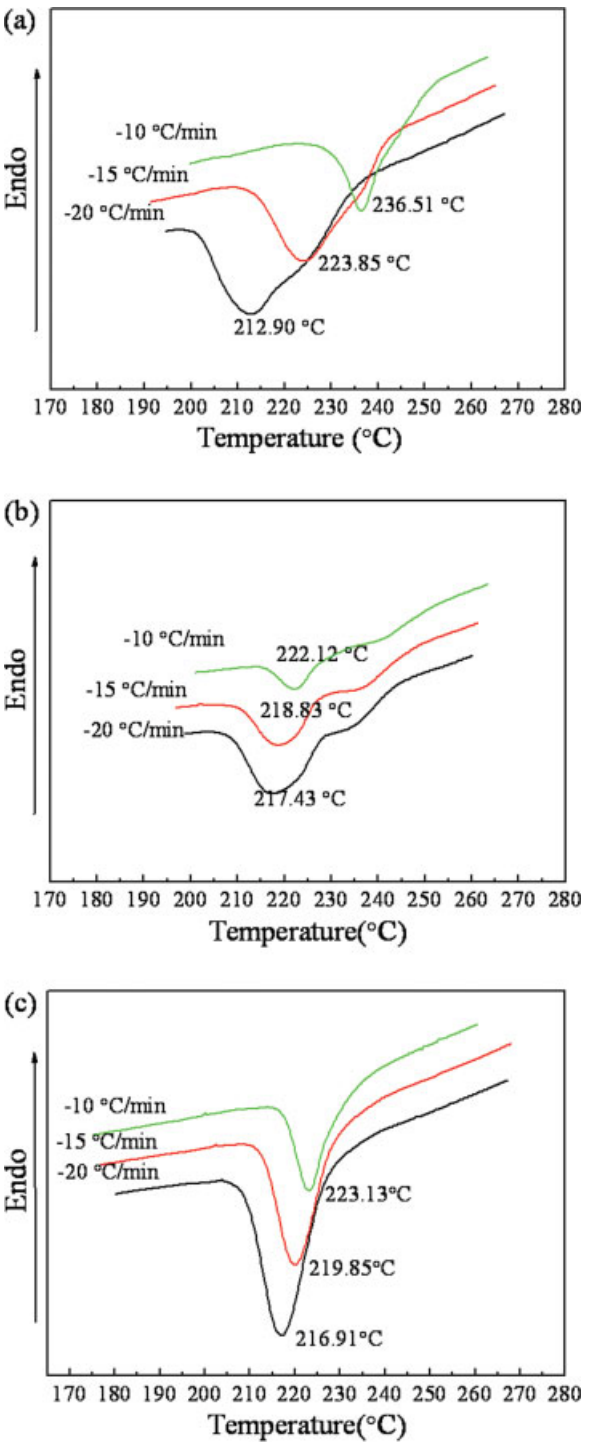

Figure 3 DSC cooling traces at predetermined cooling rates for (a) neat PPS, (b) a PA66/PPS blend, and (c) an EMA/PA66/PPS blend. [Color figure can be viewed in the online issue, which is available at www.interscience.wiley.com.]

20, 15, and 10°C/min, respectively. From these DSC curves, one can see that the exothermic crystallization peaks for both PPS and the EMA/PA66/PPS blend are monomodal, whereas for the PA66/PPS blend, they are multimodal. Apparently, the higher small

TABLE I
Crystallization Parameters Obtained from DSC Curves

Sample		PPS	PA66/PPS	EMA/PA66/PPS
10°C/min	T_p (°C)	236.51	222.12	223.13
	T_o (°C)	253.86	254.81	237.13
	t_{max} (min)	3.09	4.09	2.32
15°C/min	T_p (°C)	223.85	218.83	219.85
	T_o (°C)	245.6	250.60	233.35
	t_{max} (min)	2.45	3.20	1.85
20°C/min	T_p (°C)	212.90	217.43	216.91
	T_o (°C)	239.22	248.78	230.89
	t_{max} (min)	2.08	2.25	1.35

crystallization peak corresponds to PPS, and the lower crystallization peak corresponds to the simultaneous crystallization of PA66 and PPS because the ranges of the crystallization temperatures for the two polymers are so close. This is because the crystallization of PA66 is induced by the crystallites of PPS, and this leads to the partial overlap of crystallization for the two polymers.

From these curves, some parameters of nonisothermal crystallization for PPS and its blend, such as the onset temperature (T_o), peak or maximum crystallization temperature (T_p), and maximum crystallization time (t_{max}; i.e., the time required to crystallize completely), are available, as shown in Table I. The crystallization peak shifts to the lower temperature when the constant cooling rate is increased, whereas T_o, T_p, and t_{max} decrease; this indicates the retarded effect of the cooling rate on the nonisothermal crystallization of PPS. In the case of the PA66/PPS blend, T_o is a little higher than that of neat PPS, showing that the presence of PA66 promotes the nucleation of PPS. On the contrary, T_p is lower than that of neat PPS but higher than that of neat PA66, indicating that PPS acts as a nucleating agent for PA66 crystallization, whereas for the EMA/PA66/PPS blend, T_o and T_p of the PPS phase are lower than those of neat PPS. t_{max} is less than that of neat PPS, and this shows that EMA markedly accelerates the overall nonisothermal crystallization rate of PPS. However, compared with that of the PA66/PPS blend, T_p of the PPS phase shows little difference. The most interesting difference is that only one crystallization peak occurs: the higher small crystallization peak disappears, and this shows that the crystallization of PPS is completely overlapped by that of PA66 because of the presence of EMA. On the basis of these results, it can be concluded that the nonisothermal crystallization of PPS is greatly influenced by PA66, and in the course of nonisothermal crystallization, PA66 can induce the nucleation of PPS. In addition, the addition of EMA greatly changes the nonisothermal crystallization process of PPS and accelerates the overall crystallization rate of PPS. This is because the compatibilizer EMA modifies the interfacial interplay of the PA66/PPS blend, and this results in the complete overlap of crystallization for the two polymers.

Crystallization morphology of EMA/PA66/PPS blends

Nonisothermal crystallization morphology

The nonisothermal crystallization morphology of neat PPS, a PA66/PPS blend, and an EMA/PA66/PPS blend at a predetermined cooling rate of 15°C/min is presented in Figure 4. It can be seen from Figure 4(a) that the neat PPS can form a spherulite structure, and the diameter of the spherulite can reach about 30 μm. In the case of the PA66/PPS blend and EMA/PA66/PPS blend, one can see that no spherulite structure can be observed under the polarized optical field. This phenomenon can be ascribed to the formation of numerous small nuclei, which result from the presence of PA66. Thus, the nonisothermal crystallization of PPS is greatly influenced by PA66 and especially the addition of compatibilizer EMA.

Isothermal crystallization morphology

Optical micrographs of PPS isothermally crystallized at 250°C from the melt are presented in Figure 5. The crystalline morphology of PPS is mainly spherulite, and a Maltese cross can be observed under an orthogonally polarized optical field in the initial crystallization process [Fig. 5(b)]. The spherulite diameter can reach about 10–30 μm when the crystallization process is completed. However, with the crystallization time increasing, the spherulite superstructure is not clear anymore because the great nucleation density leads to the overlapping of spherulites.

The crystalline morphologies of PPS blended with PA66 at a concentration of 30 wt % are shown in Figure 6. The spherulite superstructure of PPS can be observed under the optical microscope, and the spherulite diameter may reach about 100 μm when isothermally crystallized at 250°C for 12 min from the melt. However, a Maltese cross cannot be observed under the orthogonally polarized optical field during the overall crystallization process. In particular, the impingement line of spherulites cannot be observed, and the spherulite superstructure disappears when the crystallization process is completed [Fig. 6(c)]. In addition, a lot of small crystals of PA66, which fill in the middle of lamellae crystals of PPS, can be observed, and this is believed to cause the extinct phenomenon mentioned previously. As is well known, PA66 is a semicrystallizable polymer, and its crystallization temperature is about 208°C (known from DSC data), a little lower than that of PPS. PA66 begins to crystallize too when PPS crystallizes at 250°C, and this shows that the presence of PPS indu-

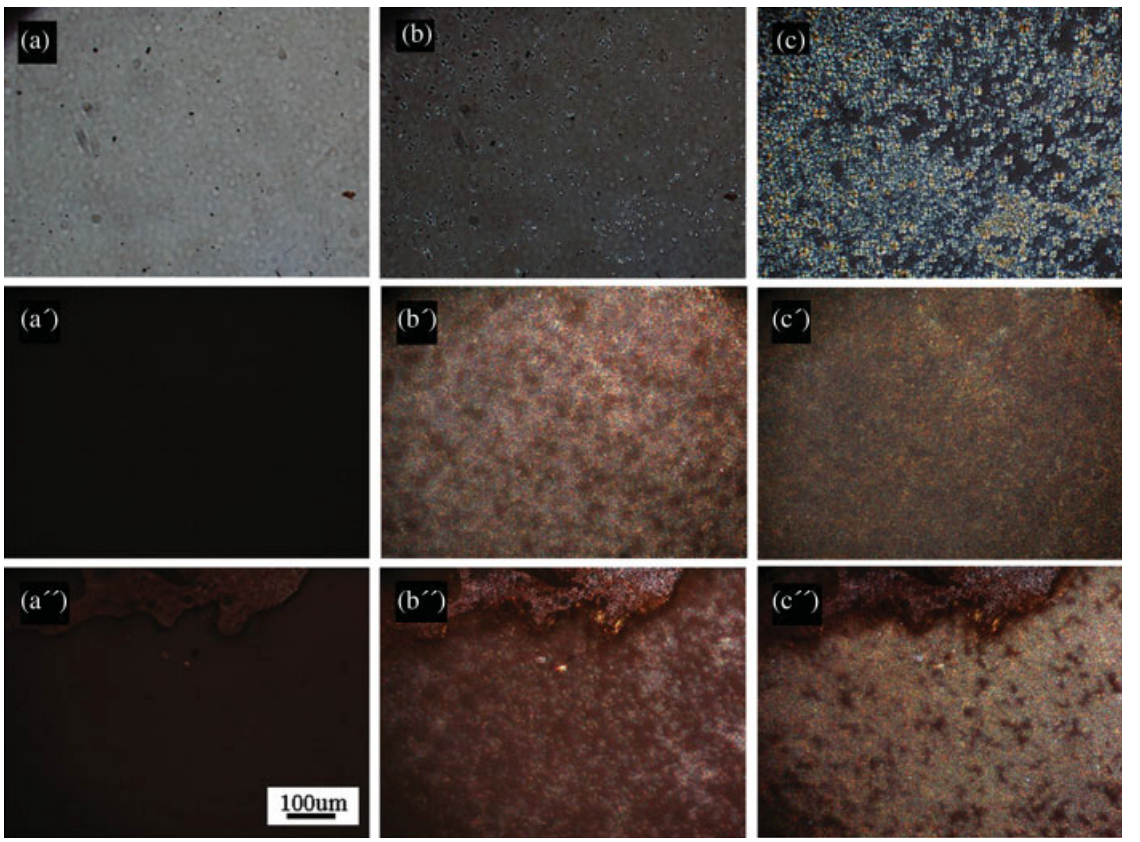

Figure 4 Nonisothermal crystallization optical micrographs at a rate of −15°C/min for (a–c) neat PPS, (a′–c′) PA66/PPS, and (a″–c″) EMA/PA66/PPS. [Color figure can be viewed in the online issue, which is available at www.interscience.wiley.com.]

ces the crystallization nucleation of PA66. In addition, Figure 6 shows that the nucleation density of PPS in its blend is lower than that of pure PPS. These results indicate that the presence of PA66 dilutes the volume of PPS, and this decreases the nucleation rate of PPS.

Figure 7 shows optical micrographs of PPS blended with PA66 by the use of compatibilizer EMA and isothermally crystallized at 240°C from the melt. One can see that the crystalline morphologies of PPS are not spherulite, and optical character cannot be observed. Numerous nuclei can be observed under the polarized optical microscope. The crystal of PA66, as shown in Figure 6, is dispersed in the middle of the PPS crystal. These results indicate that EMA has a great influence on the crystalline morphology of PPS. For one thing, EMA greatly modifies the interfacial interplay of the PA66/PPS blend, and this results in the cocrystallization of the two polymers. Moreover, the nucleation rate of the PPS phase is markedly accelerated by EMA. This is because EMA modifies the intermolecular interplay of the two polymers, and this promotes the formation of numerous stable nuclei of PPS.

According to recent literature,[27–39] the crystallization process of immiscible polymer blends for two crystalline polymers is greatly affected by the crystal-

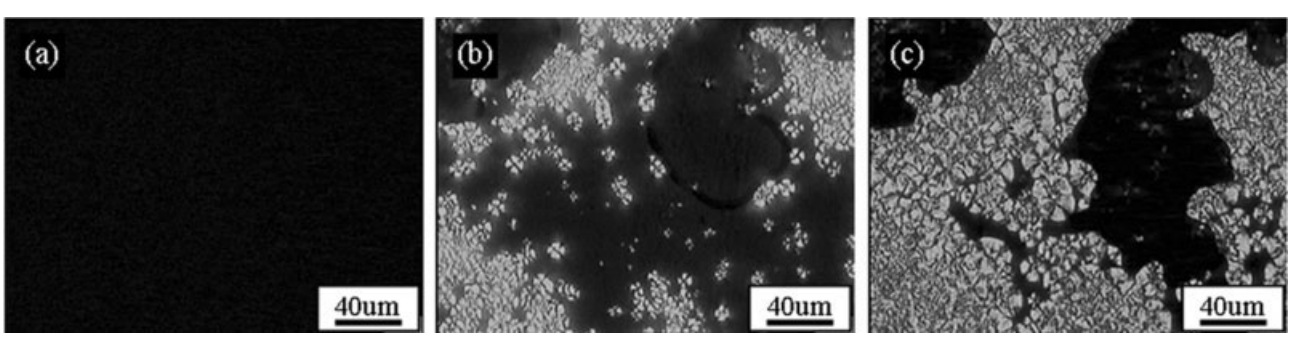

Figure 5 Optical micrographs of neat PPS isothermally crystallized at 250°C for (a) 0, (b) 5, and (c) 12 min.

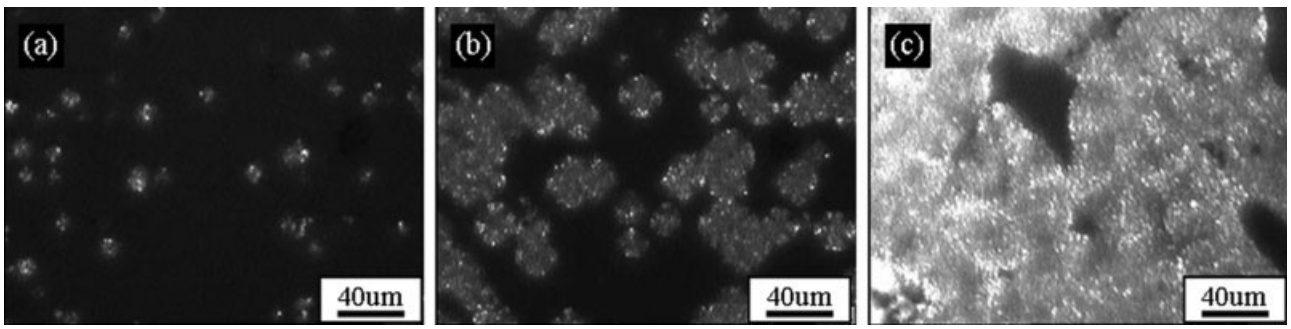

Figure 6 Optical micrographs of PA66/PPS isothermally crystallized at 250°C for (a) 3, (b) 7, and (c) 18 min.

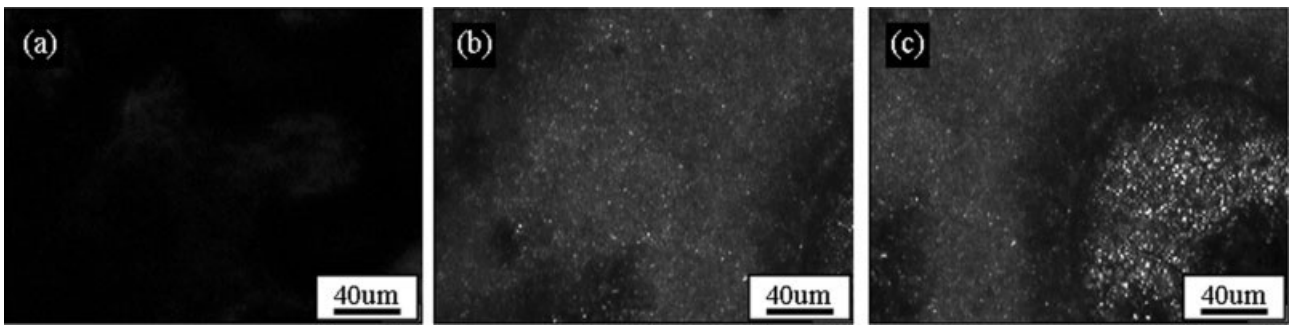

Figure 7 Optical micrographs of EMA/PA66/PPS isothermally crystallized at 250°C for (a) 0, (b) 3, and (c) 86 min.

linity, the glass-transition temperature, the melting point temperature, and the temperature range of the crystallization of the two components. On the basis of the crystallizability of the individual component polymers, here PA66 and PPS, the polymers may crystallize concurrently or sequentially if the crystallization temperatures are comparable. The presence of a second component affects both the nucleation and crystal growth of the crystallizing polymer PPS, thereby modifying the morphology and mechanical properties of PPS.

CONCLUSIONS

The crystalline morphology and nonisothermal crystallization behavior of PPS and its blend with PA66 have been investigated. The presence of PA66 greatly influences the crystallization process of PPS. The nucleation and crystallization rate of PPS is markedly accelerated by PA66. PA66 acts as a nucleating agent and changes the crystallization mechanism of PPS from homogeneous nucleation to heterogeneous nucleation. Also, the addition of compatibilizer EMA improves the compatibility of the PA66/PPS blend, accelerates the nonisothermal crystallization rate of the PPS phase, and modifies the intermolecular interplay of the two polymers, and this promotes the formation of numerous stable nuclei of PPS.

References

1. Hill, H. W.; Brady, D. G. Polym Eng Sci 1976, 16, 831.
2. Hartness, J. T. J. Natl SAMPE Symp Exhibition 1980, 6, 376.
3. Brady, D. G. Appl Polym Symp 1981, 36, 231.
4. Golovoy, A.; Mazich, K. A.; Cheung, M. F. Polym Bull 1989, 22, 175.
5. Nadkarni, V. M.; Jog, J. P. J Appl Polym Sci 1986, 32, 5817.
6. Shingankuli, V. L.; Jog, J. P.; Nadkarni, V. M. J Appl Polym Sci 1988, 36, 335.
7. Akhtar, S.; White, J. L. Polym Eng Sci 1991, 31, 84.
8. Akhtar, S.; White, J. L. Polym Eng Sci 1992, 32, 690.
9. Cheung, M. F.; Golovoy, A.; Mindroiu, V. E. Polymer 1993, 34, 3809.
10. Masamoto, J.; Kubo, K. Polym Eng Sci 1996, 36, 265.
11. Hanley, S. J.; Rafalko, J. J.; Steele, K. A. J Polym Sci Part A: Polym Chem 1999, 37, 3473.
12. Harmia, T.; Friedrich, K. Plast Compos Sci Technol 1995, 53, 423.
13. Harmia, T.; Friedrich, K. Plast Rubber Compos Process Appl 1995, 23, 63.
14. Huang, C. C.; Chang, F. C. Polymer 1997, 38, 4287.
15. Muratoglu, O. K.; Argon, A. S.; Cohen, R. E. Polymer 1995, 36, 4771.
16. Li, Z. M.; Li, L. B.; Shen, K. Z. Polymer 2005, 46, 5358.
17. Li, Z. M.; Li, L. B.; Shen, K. Z. Macromol Rapid Commun 2004, 25, 553.
18. Quan, H.; Li, Z. M.; Yang, M. B. Compos Sci Technol 2005, 65, 999.
19. Lee, B. S.; Chun, B. C. Polym Compos 2003, 24, 192.
20. Zou, H.; Zhang, Q.; Tan, H.; Wang, K.; Du, R. N.; Fu, Q. Polymer 2006, 47, 6.
21. Zou, H.; Wang, K.; Zhang, Q.; Fu, Q. Polymer 2006, 47, 7821.

22. Chen, Z. B.; Liu, X. J.; Lu, R. G.; Li, T. S. J Appl Polym Sci 2006, 101, 969.
23. Chen, Z. B.; Liu, X. J.; Lu, R. G.; Li, T. S. J Appl Polym Sci 2006, 102, 523.
24. Han, C. D.; Chuang, H. K. J Appl Polym Sci 1985, 30, 4431.
25. Han, C. D.; Kim, J. K. Macromolecules 1989, 22, 1914.
26. Han, C. D.; Kim, J. K. Macromolecules 1989, 22, 4292.
27. Nadkarni, V. M.; Jop, J. P. In Two-Phase Polymer Systems; Utracki, L. A., Ed.; Hanser: Berlin, 1991; p 213.
28. Lotti, N.; Pizzoli, M.; Ceccorulli, G.; Scandola, M. Polymer 1993, 34, 4935.
29. Dufresne, A.; Vincendon, M. Macromolecules 2000, 33, 2998.
30. Blumm, E.; Owen, A. J. Polymer 1995, 36, 4077.
31. Avella, M.; Martuscelli, E.; Orsello, G.; Raimo, M.; Pascucci, B. Polymer 1997, 38, 6135.
32. Qiu, Z. B.; Ikehara, T.; Nishi, T. Polymer 2003, 44, 3101.
33. Qiu, Z. B.; Ikehara, T.; Nishi, T. Polymer 2003, 44, 7519.
34. Qiu, Z. B.; Ikehara, T.; Nishi, T. Polymer 2003, 44, 2503.
35. Qiu, Z. B.; Ikehara, T.; Nishi, T. Polymer 2005, 46, 11814.
36. Qiu, Z. B.; Ikehara, T.; Nishi, T. Polymer 2003, 44, 7749.
37. Zhong, G. J.; Li, Z. M. Polym Eng Sci 2005, 45, 1655.
38. Zhong, G. J.; Li, L. B.; Li, Z. M. Macromolecules 2006, 39, 6771.
39. Li, Z. M.; Qian, Z. Q.; Yang, M. B. Polymer 2005, 46, 10466.